

Dry-Mass Sensing for Microfluidics

T. Müller,¹ D. A. White,¹ and T. P. J. Knowles^{1, a)}

Department of Chemistry, University of Cambridge, Lensfield Road, Cambridge CB2 1EW, United Kingdom

(Dated: 25 November 2014)

We present an approach for interfacing an electromechanical sensor with a microfluidic device for the accurate quantification of the dry mass of analytes within microchannels. We show that depositing solutes onto the active surface of a quartz crystal microbalance by means of an on-chip microfluidic spray nozzle and subsequent solvent removal provides the basis for the real-time determination of dry solute mass. Moreover, this detection scheme does not suffer from the decrease in the sensor's quality factor and the viscous drag present if the measurement is performed in a liquid environment, yet allows solutions to be analysed. We demonstrate the sensitivity and reliability of our approach by controlled deposition of nanogram levels of salt and protein from a micrometer-sized channel.

PACS numbers: 73.23.Hk, 07.50.Qx, 85.35.Be

Keywords: Microfluidics, Mass measurement, Electromechanical transducers, QCM

Label-free, quantitative detection of small quantities of biomolecules underlies experimental approaches in industrial, applied, as well as basic research in numerous fields ranging from physics and chemistry to biology, food science and medicine.¹⁻⁵ In such applications, microfluidic strategies⁶⁻⁸ allow for an enhanced level of control over the specific environment⁹ and offer a wide range of preparation and separation techniques.¹⁰⁻¹⁴ The ability for accurate label-free measurements in micro technology platforms opens up fruitful possibilities for multidisciplinary research and has the propensity to advance our understanding of biology as well as offer exciting perspectives for the development of bio-inspired nanomaterials.¹⁵⁻²⁰

To fulfill the demands of the growing complexity of these analyte systems, there is currently a pressing need for multi-purpose, high-sensitivity measurement strategies. We approach this challenge by combining the versatility of microfluidics with the precision of electromechanical sensors (EMS), without the impediment of the substantial decrease of the resonator quality factor in liquid. Utilising EMS as detectors is highly attractive in terms of ease of use and cost. Furthermore, while electromechanical transducers do not provide any information directly about the charge-to-size ratio, which is available from mass-spectrometry,²¹ they are independent of ionisation energies and can therefore yield quantitative results on the total mass. Moreover, interfacing with microfluidic continuous flow separation techniques^{12,13} in principle could allow for determination of a large variety of physical properties of biomolecules in solution such as size or charge.

More specifically, we have developed an ex-situ detection method consisting of a microfluidic chip interfaced with a quartz crystal microbalance (QCM) measuring the dry mass of the microchannel's contents. In practice, the analyte within the chip is deposited onto the active sur-

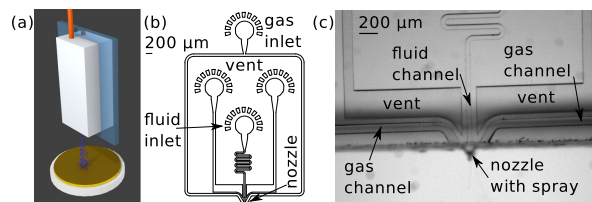


FIG. 1. (a) Schematic representation of the measurement setup consisting of a microfluidic device spraying a controlled volume of a solution onto the gold electrode of a quartz crystal microbalance. (b) Design of a microfluidic nozzle. (c) Micrograph of a spraying device with a continuous flow rate set to 1 ml/h and an exposure time of 30 μ s. The scale bars are 200 μ m.

face of the microelectromechanical sensor through a microfluidic nozzle^{22,23} driven by pressurised gas co-flowing with the liquid at end of the channel.²⁴ This scheme is depicted in Fig. 1(a) and a micrograph of the spray nozzle in action is shown in Fig. 1(b).

To allow for quantitative analysis of the solute inside the channel, the solvents impinging on the microbalance need to be evaporated completely. This objective has been effected in macroscopic approaches by stopping flow and heating the sensor electrodes²⁵ or by immersing the analyte in supercritical fluids.²⁶ In our integrated microscopic strategy, a mechanical shutter prevents deposition while it is closed, permitting *continuous* operation of the microfluidic device resulting in very accurate flow from the nozzle. It should be noted that our approach effectively decouples the processing and measurement stages, and thus benefits from the optimal performance of both integral parts. In particular, combination with microfluidic separative methods - such as diffusive or electrophoretic migration - in the incorporated microfluidic device would provide specificity to our detection module, creating a simple, highly sensitive and versatile microanalytical platform in the shape of a “lab on two chips”. In such an approach, separation occurs in so-

^{a)} Electronic mail: tpjk2@cam.ac.uk

lution whereas the measurement is performed in air, significantly enhancing applicability and sensitivity as the quality factor of the resonator is not adversely affected by viscous drag.

Quartz crystal microbalances are an established technique for the determination of mass,^{27,28} and there is also a variety of electro- and purely mechanical sensors operating in a macroscopic liquid environment^{29–34} as well as *inside* microfluidic devices^{35–39} or containing microfluidic channels themselves.^{40,41} While these latter approaches yield good results in terms of sensitivity, the operation of QCMs in liquid suffers from the reduction in their quality factor due to viscous damping and quantitative measurement of (dry) mass remains challenging. In our “lab-on-two-chips” approach the automated two-step operation - deposition of analyte and subsequent evaporation of solvents utilising a mechanical shutter - allows for simple, continuous operation and enables us to straightforwardly access the analyte’s dry mass.

Microfluidic devices were fabricated to a height of 25 μm using standard soft lithography techniques in polydimethylsiloxane (PDMS, Sylgard 184, Dow Corning, Midland MI, USA) on SU8 masters.⁴² As can be seen in Fig. 1(b) the device contains a 10 μm wide horizontal line at the nozzle ensuring reproducible fabrication. This template line can be used to position a razor blade to cut the device at the exact position of the nozzle. Upon plasma activation of the PDMS devices and the microscope glass slides, the edge of the glass slide can be aligned to the edge of the device by pressing the side of a razor blade (or similarly flat object) laterally to the pdms and placing the glass slide on top, also pressing it against the blade. Prior to operation the sealed devices were rinsed with aquapel (Pittsburgh Glass Works, Pittsburgh PA, USA) to apply a hydrophobic coating to the PDMS.

Using a syringe pump (Harvard Apparatus PHD2000) and precision glass syringes (Hamilton Bonaduz gastight 1700 and 1800 series with volumes between 50 and 1000 μl) connected via polyethylene tubing (Smiths Medical, 800/100/120), a controlled flow of liquid is driven through the fluid inlet (marked in Fig. 2(b)) of a microfluidic channel. This channel is open at the edge of the glass slide where it is met by two further channels at an angle of 60 degrees (see Figs. 1(b) and (c)) through which pressurised nitrogen gas at ca. 4 bar is applied, forming a microfluidic spray nozzle. We found that the reliability of continuous operation of this design could be enhanced considerably by fabricating on the same chip a set of vented channels between the liquid and gas channels to prevent the gas from being transported into the fluidic channel due to the gas-permeable nature of PDMS.

The solute is deposited on the microbalance’s active surface through a microfluidic nozzle at which a spray is formed via pressurised gas.²² A schematic representation thereof is shown in Fig. 1(a). Alternatively, an electro-spray could be generated⁴³ or a glass capillary could be attached to the analysis outlet of an existing device, at

the end of which a gas flow creates a spray. The latter approach would allow for straightforward incorporation into multifunctional microfluidic systems.

To obtain absolute values of the mass deposited in this manner, a calibration measurement can be carried out by spraying ions of a known concentration onto the balance and determining the ensuing shift in resonance frequency.

In order to evaporate all liquid from the spray and to equilibrate the QCM, a shutter controlled with a stepper motor is closed for 19.5 s after 0.5 s of spraying. Furthermore, to protect the sensitive apparatus from fast temperature fluctuations and air currents the microbalance and the microfluidic chip were placed in an incubator casing (with the temperature control turned off). Alignment between the microbalance and the chip is achieved by a “helping hand” clamp holder which allows for simple positioning of the microfluidic chip with respect to the QCM. However, incorporation of a *xyz*-micrometer stage with coordinates relative to the centre of the quartz chip is readily achievable.

Readout of the QCM crystal (Stanford Research Systems 100RX1, Cr/Au, 5 MHz) is performed with a commercial frequency counter (Stanford Research Systems QCM200) at a gate time of 1 s, leading to an accuracy of 0.1 Hz. The sensor has an electrode surface of 1.37 cm^2 , with its active area confined to 0.40 cm^2 by the geometry of the second electrode, and a mass sensitivity coefficient of 0.0566 Hz/ng.

After each experimental run, the microbalance was unmounted and rinsed with deionised water to remove adsorbed solutes, which recovered its original properties.

In Fig. 2(a) the functionality and reliability of this approach is demonstrated. Shown is the frequency shift of a 5 MHz quartz crystal microbalance upon the controlled deposition of 10 mM NaCl solution. By initiating the flow of the solution and opening the shutter for a time period of $t = 500$ ms, a pre-defined volume of solution is sprayed onto the balance. This deposited mass is determined by $m = Q \cdot t \cdot M$, with Q being the volume flow rate and M being the molar mass of the compound, and results in a downward spike in the reading of the QCM’s resonance frequency. After all liquid has evaporated, the frequency reading saturates at a value shifted with respect to the original one corresponding to the mass of the solute deposited. Flow rates of 250, 150 and 100 $\mu\text{l}/\text{h}$ were applied, yielding volumes of 35, 21 and 14 nl or masses of 20, 12 and 8 ng, respectively, per 0.5 s spray burst - well below the limit of micropipettes.

Our results show that the equilibrated values of the frequency shifts - resulting from repeated cycles of solution deposition and solvent removal - display a remarkably linear relationship, the slope of which is proportional to the flow rate and stable over tens of minutes. Upon stopping the flow, a well-defined base-line is rapidly attained after a short settling time of the order of a minute due to the change in temperature caused by the ceased evaporative cooling. These measurements demonstrate a dynamic range of over three orders of magnitude for

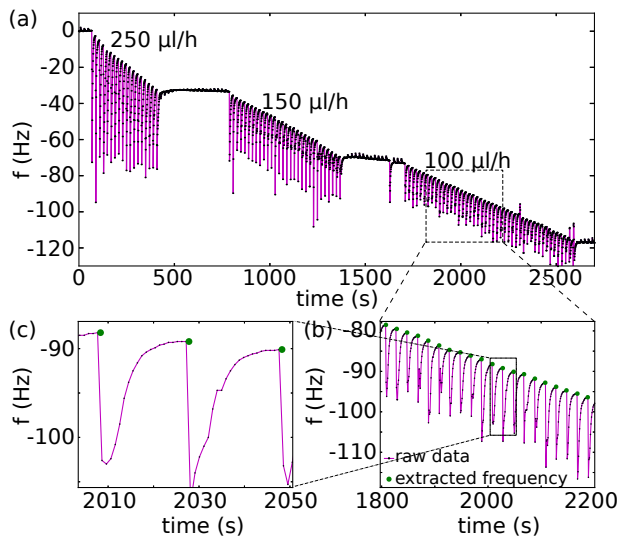


FIG. 2. (a) Measured frequency shift as a function of time for the deposition of a 10 mM NaCl solution at three different flow rates. A shutter controls spraying during 0.5 s followed by 19.5 s for drying and equilibration, leading to the sharp flanks and subsequent settling of the resonance frequency. (b) Magnification of a part of (a) with the flow rate set to 100 $\mu\text{l/h}$. The green dots represent the maximum frequency within each 20 s interval. (c) Zoom on individual spray bursts from (a) and (b).

the detected mass, from nanograms to micrograms. The linear response is maintained up to a point where several micrograms of solutes have been deposited during continuous operation over time scales exceeding thousands of seconds. In a small fraction of cases, an individual spray burst was observed to result in a transient peak that increased rather than decreased the resonance frequency. However, upon evaporation the overall negative frequency shift was restored. Such spikes can be removed readily with a suitable data-processing algorithm which is checking the direction of the frequency shift upon deposition.

A detailed analysis of several consecutive spray bursts (Figs. 2(b) and (c)) shows even more clearly the precision obtained with the presented approach. Here, the green dots are the extracted frequency reading obtained by taking the maximum frequency within a 20 s interval. Readout noise could be further reduced by synchronising the frequency measurement with the shutter opening or using a flank-detection algorithm and averaging the last few frequency points before the shutter is reopened.

To illustrate further the precision of this method, we have recorded the frequency shift due to the deposition of 1 mg/ml of the model protein lysozyme (without NaCl) at a flow rate of 100 $\mu\text{l/h}$ - i.e., continuously spraying 100 $\mu\text{g/h}$, 2.5 $\mu\text{g/h}$ of which are deposited on the QCM - over 2 h (see Fig. 3(a)). A linear response is conserved during the entire measurement period. In Fig. 3(b) the resulting frequency shift of 200 individual spray burst is

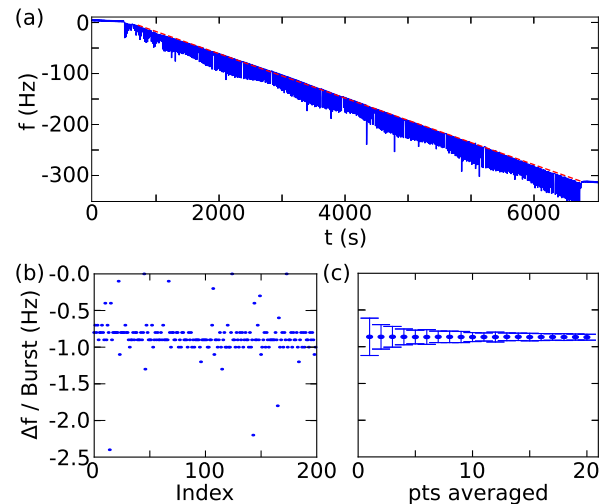


FIG. 3. (a) Spray deposition of lysozyme at a concentration of 1 mg/ml over a time scale of 2 hours with a shutter opening time of 0.5 s every 20 s and a flow rate of 100 $\mu\text{l/h}$. The dashed red line is a guide to the eye. (b) Scatter plot of the frequency shift of the central 200 individual burst in (a). Note that the detector circuit's gate time of 1 s leads a frequency resolution of 0.1 Hz. (c) Average frequency shift and corresponding standard deviation per burst when averaging over consecutive points.

shown. It can be seen that most of the bursts result in a shift of between -0.7 to -1.0 Hz, with minute drift of around -0.05 Hz/h and just a dozen points above and below this window in a range of 0 to -2.4 Hz. These outliers might result from ambient influences that can interfere with the spray deposition, inaccuracies in the shutter opening time, or combinations thereof. Averaging the frequency shifts of a small number of consecutive bursts - as presented in Fig. 3(c) - naturally decreases the standard deviation of this average signal, with values ranging from ± 0.25 Hz without averaging over ± 0.09 Hz for 5 points to ± 0.04 Hz for 20 averages. For the remainder of this work we have chosen to average over 5 points as a compromise between small amount of mass per averaged value and superior signal-to-noise ratio.

To benchmark the performance of this technique the frequency shift resulting from a 500 ms spray burst is presented as a function of deposited mass in Fig. 4. The sprayed mass has been calculated from the volume of liquid flowing through the device in 0.5 s and the pre-set concentration of analyte ranging from 1 to 10 mM and 1 mg/ml NaCl (filled symbols) as well as 0.1 and 1 mg/ml lysozyme (without any salt; empty symbols). The frequency values shown are the mean and standard deviations taken from tens to hundreds of spray bursts averaged over five consecutive shutter openings.

The data shown are taken with 3 nominally identical devices (different symbols), with one device studied at two different relative alignments of the nozzle with respect to the QCM (different colours), resulting in 4

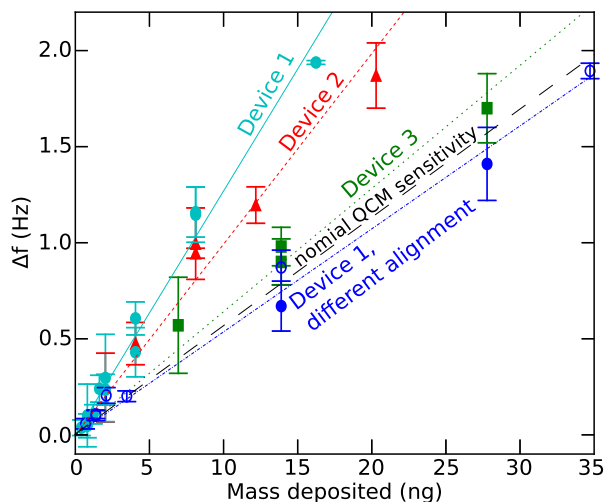


FIG. 4. Measured frequency shift per 0.5 s spray burst averaged over 5 consecutive bursts as a function of actual mass deposited. The data are for 3 different devices (device 1: circles, device 2: triangles, device 3: squares) with different alignments represented by different colours and using predetermined concentrations of NaCl (filled symbols) and lysozyme (hollow symbols). The lines are fits to each of the individual data sets.

distinct data sets. We note that for each data set the different flow rates and analyte concentrations yield frequency shifts that are linearly proportional to the mass deposited. Thus we are able to first calibrate our measurement setup using a well-defined analyte concentration and consequently measure unknown amounts of solute to a high degree of accuracy. It is thus possible to achieve nanogram precision using minute sample quantities. The slopes can vary up to roughly a factor of two between experimental runs due to the alignment of spray nozzle and microbalance in combination with the non-uniform mass sensitivity of the QCM. In particular, a well-aligned device - where the spray hits the microbalance centrally - can exceed the average nominal sensitivity of the QCM (widely-dashed black line). By measuring accurately the position of the spray deposited, the expected frequency shift per unit mass could in principle be calculated precisely.⁴⁴ Since we can calibrate the mass sensitivity by running a solution with well-known concentration first, such a cumbersome process is, in fact, unnecessary.

Our measurements show that 5 bursts of as little as a few nanograms of deposited mass each are enough for the precise determination of the analyte concentration within a microfluidic channel. Thus, we have demonstrated an accurate and quantitative label-free detection method for microfluidic technologies by exploiting the high sensitivity of a commercially available quartz crystal microbalance (0.0566 Hz/ng).

Traditional microfluidic methods work with the microelectromechanical sensor placed in liquid or at a liquid-air

interface. Therefore these techniques are heavily affected by viscous drag of particles in liquid, and consequently they are not able to quantitatively resolve the dry mass of the analyte. Moreover, these strategies require the surface of the sensor to be functionalised in order to guarantee adherence of the sample molecules.^{45,46} The approach discussed here circumvents both of these difficulties by transporting the analyte out of the channel and onto the sensor, where it is dried. Once all solution has evaporated - a process that is automatically taking place while a mechanical shutter decouples the continuous spray from the sensor - gravitation and surface adhesion hold all solutes in place. Nevertheless, if desired, specificity could in principle be recovered at the price of generality by functionalising the QCM surface in combination with a washing step after every spray burst.

The detection method described in the present paper provides a highly accurate and versatile tool for quantitative assays. Measurements of analyte mass have proved to be highly successful in other areas of analytical chemistry, and the integration between EMS and microfluidics opens up the possibility of quantitative mass measurements in a format that is compatible with conventional PDMS microfluidics. Crucially, the approach for mass measurement discussed in the present work is not dependent on the surface chemistry of the sensor nor on specific binding events, requirements that underlie conventional use of QCMs in liquid. This approach therefore represents a label-free detection module that is applicable to volumes and concentrations that are of interest to lab on a chip applications. In order to fully harness the potential of this measurement strategy using complex analytes - such as biological samples - the detection module could be coupled to microfluidic upstream separation techniques such as diffusive filtering¹⁰ or free-flow electrophoresis.^{12,13}

We thank Alexander K. Buell, Igor Efimov, and Victor Ostanin for valuable discussions on QCM sensors and gratefully acknowledge financial support from the Swiss National Science Foundation (SNF), the Engineering and Physical Sciences Research Council (EPSRC), the Biotechnology and Biological Sciences Research Council (BBSRC), the European Research Council (ERC), as well as the Frances and Augustus Newman Foundation. Part of the work described here has been the subject of a patent application²⁴ filed by Cambridge Enterprise.

¹S. Jones and J. M. Thornton, *Proc Natl Acad Sci USA*, 1996, **93**, 13–20

²A. L. Fink, *Folding and Design*, 1998, **3**, R9 – R23

³F. Chiti and C. M. Dobson, *Annu Rev Biochem*, 2006, **75**, 333–366

⁴J. Ubbink, A. Burbidge and R. Mezzenga, *Soft Matter*, 2008, **4**, 1569–1581

⁵A. Aguzzi and T. O'Connor, *Nat Rev Drug Disc*, 2010, **9**, 237–248

⁶G. M. Whitesides, *Nature*, 2006, **442**, 368–373

⁷C. A. Baker, C. T. Duong, A. Grimley and M. G. Roper, *Bioanalysis*, 2009, **1**, 967–975

⁸J. Wu and M. Gu, *J Biomed Opt*, 2011, **16**, 080901–080901

- ⁹V. Foder, S. Pagliara, O. Otto, U. F. Keyser and A. M. Donald, *J Phys Chem Lett*, 2012, **3**, 2803–2807
- ¹⁰J. P. Brody and P. Yager, *Sens Act A*, 1997, **58**, 13–18
- ¹¹K. Ahn, C. Kerbage, T. P. Hunt, R. Westervelt, D. R. Link and D. Weitz, *Appl Phys Lett*, 2006, **88**, 024104–024104
- ¹²N. Pamme, *Lab Chip*, 2007, **7**, 1644–1659
- ¹³A. Lenshof and T. Laurell, *Chem Soc Rev*, 2010, **39**, 1203–1217
- ¹⁴A. Abate, J. Agresti and D. Weitz, *Appl Phys Lett*, 2010, **96**, 203509
- ¹⁵D. M. Fowler, A. V. Koulov, C. Alory-Jost, M. S. Marks, W. E. Balch and J. W. Kelly, *PLoS Biol*, 2006, **4**, e6
- ¹⁶D. M. Fowler, A. V. Koulov, W. E. Balch and J. W. Kelly, *Trends Biochem Sci*, 2007, **32**, 217–224
- ¹⁷D. Otzen, *Prion*, 2010, **4**, 256–264
- ¹⁸J. Aizenberg, *MRS Bulletin*, 2010, **35**, 323–330
- ¹⁹T. P. J. Knowles and M. J. Buehler, *Nat Nanotechnol*, 2011, **6**, 469–479
- ²⁰F. J. H. Hol and C. Dekker, *Science*, 2014, **346**, 1251821
- ²¹T. Sikanen, S. Franssila, T. J. Kauppila, R. Kostianen, T. Kotiaho and R. A. Ketola, *Mass Spectrometry Reviews*, 2010, **29**, 351–391
- ²²J. Thiele, M. Windbergs, A. R. Abate, M. Trebbin, H. C. Shum, S. Forster and D. A. Weitz, *Lab Chip*, 2011, **11**, 2362–2368
- ²³E. Amstad, C. Holtze and D. A. Wietz, *PCT International Application No. 61/733,604*, 2012
- ²⁴T. Müller, D. A. White and T. P. J. Knowles, *GB Patent Appl No. 1320127.2*, 2013
- ²⁵W. W. Schulz and W. H. King, *J Chromatogr Sci*, 1973, **11**, 343–348
- ²⁶E. S. di Milia, D. A. Gleichauf and T. E. Whiting, *US Patent 5369033*, 1992
- ²⁷G. Sauerbrey, *Zeitschrift f. Physik A*, 1959, **155**, 206–222
- ²⁸J. Hlavay and G. G. Guilbault, *Anal Chem*, 1977, **49**, 1890–1898
- ²⁹K. K. Kanazawa and J. G. Gordon II, *Anal Chim Acta*, 1985, **175**, 99–105
- ³⁰J. Rickert, A. Brecht and W. Göpel, *Anal Chem*, 1997, **69**, 1441–1448
- ³¹M. E. Welland, C. M. Dobson and T. P. J. Knowles, *Int Patent Appl WO2007132211 A1*, 2007
- ³²M. B. Hovgaard, M. Dong, D. E. Otzen and F. Besenbacher, *Biophys J*, 2007, **93**, 2162–2169
- ³³T. P. J. Knowles, W. Shu, G. L. Devlin, S. Meehan, S. Auer, C. M. Dobson and M. E. Welland, *Proc Natl Acad Sci USA*, 2007, **104**, 10016–10021
- ³⁴D. A. White, A. K. Buell, C. M. Dobson, M. E. Welland and T. P. J. Knowles, *FEBS Lett*, 2009, **583**, 2587–2592
- ³⁵B. Godber, M. Frogley, M. Rehak, A. Sleptsov, K. S. Thompson, Y. Uludag and M. A. Cooper, *Biosensors and Bioelectronics*, 2007, **22**, 2382 – 2386
- ³⁶N. Doy, G. McHale, M. I. Newton, C. Hardacre, R. Ge, J. M. MacInnes, D. Kuvshinov and R. W. Allen, *Biomicrofluidics*, 2010, **4**, 014107
- ³⁷D. Hill, N. Sandstrom, K. Gylfason, F. Carlborg, M. Karlsson, T. Haraldsson, H. Sohlstrom, A. Russom, G. Stemme, T. Claes, P. Bienstman, A. Kazmierczak, F. Dortu, M. Bauls Polo, A. Maquieira, G. M. Kresbach, L. Vivien, J. Popplewell, G. Ronan, C. Barrios and W. van der Wijngaart, Engineering in Medicine and Biology Society (EMBC), 2010 Annual International Conference of the IEEE, 2010
- ³⁸Y. F. Yu, V. Kanna, T. Bourouina, S. H. Ng, P. H. Yap and A. Q. Liu, International Conference on Micro Electro Mechanical Systems, 2010
- ³⁹R. Hu, A. C. Stevenson and C. R. Lowe, *Analyst*, 2012, **137**, 2846–2851
- ⁴⁰T. P. Burg and S. R. Manalis, *Appl Phys Lett*, 2003, **83**, 2698–2700
- ⁴¹S. S. Verbridge, J. B. Edel, S. M. Stavis, J. M. Moran-Mirabal, S. D. Allen, G. Coates and H. G. Craighead, *J Appl Phys*, 2005, **97**, 124317
- ⁴²D. C. Duffy, J. C. McDonald, O. J. A. Schueller and G. M. Whitesides, *Anal Chem*, 1998, **70**, 4974–4984
- ⁴³R. S. Ramsey and J. M. Ramsey, *Anal Chem*, 1997, **69**, 1174–1178
- ⁴⁴P. J. Cumpson and M. P. Seah, *Meas Sci Technol*, 1990, **1**, 544–555
- ⁴⁵B. D. Spangler and B. J. Tyler, *Anal Chim Acta*, 1999, **399**, 51–62
- ⁴⁶L. Nicu and T. Reichlé, *J Appl Phys*, 2008, **104**, 111101–111116